(5) and 2.223 (4) Å for the other two equatorial Ni-P distances; the equatorial P-Ni-P angles opposite the equatorial bonds are 126.7 (2), 118.8 (2), and 114.0 (2)°, respectively. In the case of $[Ni(PP_3)P(OMe)_3]^{2+}$, the distortion from ideal C_3 symmetry may result from one AsF_6^- counterion contacting with the phenyl substituents on the P111 atom, where the C···F distance is ca. 3.1 Å. The closest intramolecular contacts in **1** and **2** are between the $P(OMe)_3$ ligand oxygen atoms and the phenyl substituents on the PP_3 ligand, O···C distances ca. 3.2 Å.

As a result of the smaller covalent radius of a phosphite phosphorus atom, metal-phosphite M-P distances are generally shorter than metal-phosphine distances. The same trend is observed in these two structures. In both **1** and **2** the shortest metal-ligand distances are the metal-phosphite distances (2.105 (12) and 2.137 (2) Å, respectively). The next shortest metal-phosphorus distance in **1** and **2** is to the apical phosphorus atom, P2 (2.125 (10) and 2.182 (2) Å, respectively). The nickel to equatorial phosphorus distance, 2.294 (2) Å average, in **2** not only is the longest metal-phosphorus distance in **1** and **2** but also is unexpectedly longer than the cobalt to equatorial phosphorus distance, 2.211 (6) Å, in **1**. The Co-phosphite distance, 2.105 (12) Å, in **1** is significantly shorter than the apical and equatorial Co-phosphite distances (2.141 (5) and 2.150 (5) Å, respectively) in the distorted trigonal-bipyramidal complex $[Co(etp)(P(OMe)_3)_2]BF_4$ (etp = $PhP(CH_2CH_2PPh_2)_2$).[36] The apical and equatorial Co-phosphine distances in $[Co(etp)(P(OMe)_3)_2]BF_4$ are comparable to the Co-phosphine distances observed in this study.

Approximate cone angles measured for the trimethyl phosphite ligand in **1** and **2** are 87 and 94°, respectively (cf., Tolman cone angle of 107° for the ligand $P(OMe)_3$).[31] The 7° difference in the trimethyl phosphite cone angle between **1** and **2** is manifested in the M-P-O and O-P-O angles. The Co-P-O angle in **1** is ca. 3° larger than the average Ni-P-O angle in **2**. The O-P-O angle in **1** is ca. 4° smaller than the average O-P-O angle in **2**. The O-P and O-C distances and P-O-C angles of the trimethyl phosphite are relatively insensitive to the difference in the trimethyl phosphite cone angle between **1** and **2**. The 7° difference between the cone angle of $P(OMe)_3$ in **1** and **2** may be due to the shorter Co-$P(OMe)_3$ and Co-P_{eq} distances vs. longer Ni-$P(OMe)_3$ and Ni-P_{eq} distances. The shorter Co-P_{eq} bond lengths, ca. 0.06-0.11 Å shorter, result in the phenyl substituents on the equatorial phosphorus atoms being held closer to the Co-$P(OMe)_3$ coordination site than for the corresponding Ni-$P(OMe)_3$ coordination site. The $P(OMe)_3$ ligand is sufficiently flexible to accommodate changes in its internal geometry at the M-P-O and O-P-O angles, and it exhibits the common head-to-tail conformation found in other transition-metal complexes of trimethyl phosphite.[37] Curiously, the trimethyl phosphite ligand in **1** is coordinated in a sterically more demanding eclipsed conformation relative to the PP_3 ligand, and it appears to rotate in the same direction as the PP_3. The trimethyl phosphite in **2** is coordinated in a less sterically demanding gauche conformation and appears to turn in the opposite direction from the PP_3 ligand. Otherwise, the geometrical features of trimethyl phosphite in **1** and **2** are similar to those previously reported.[37]

Acknowledgment. The authors express appreciation to Loren Chen for assitance in obtaining some of the $^{31}P\{^1H\}$ NMR spectra, to Dr. Judith Gallucci for technical advice on the X-ray studies, to Dr. Steven Socol for helpful comments on this manuscript, and to Marietta College for a sabbatical leave to W.H.H. The research was partially supported by the University Exploratory Research Program of the Procter and Gamble Co.

Registry No. **1**, 99687-47-5; **2**, 99687-50-0; $[Co(PP_3)(PPh_2OMe)]AsF_6$, 99687-52-2; $[Co(PP_3)(PEt_3)]AsF_6$, 99687-54-4; $[Co(PP_3)(PPh_2Me)]AsF_6$, 99705-72-3; $[Ni(PP_3)(P(OEt)_3)](AsF_6)_2$, 99687-56-6; $[Ni(PP_3)(P(OCH_2CF_3)_3)](BF_4)_2$, 99687-58-8; $[Co(PP_3)CO]BF_4$, 99687-59-9; $CoCl(PP_3)$, 55297-75-1; $CoBr(PP_3)$, 55236-46-9; $CoI(PP_3)$, 55236-47-0; $Co(CN)(PP_3)$, 55236-49-2; $Co(NCS)(PP_3)$, 55236-48-1; $[Co(P(OMe)_3)_5]BF_4$, 99687-60-2; $[NiCl(PP_3)]AsF_6$, 99687-61-3; $[NiBr(PP_3)]AsF_6$, 99687-63-5; $[NiI(PP_3)]AsF_6$, 99687-65-7; $[NiH(PP_3)]AsF_6$, 99705-73-4; $[Ni(PP_3)CO](BF_4)_2$, 99687-67-9; $[Co(PP_3)(PMe(O\text{-}i\text{-}Pr)_2)]AsF_6$, 99687-69-1; $[Co(PP_3)(PF_2OMe)]AsF_6$, 99687-71-5; $[Ni(PP_3)CN]^+$, 99687-72-6; $CoH(PP_3)$, 55088-11-4.

Supplementary Material Available: Tables of hydrogen positional parameters, anisotropic thermal parameters, and observed and calculated structure factor amplitudes (42 pages). Ordering information is given on any current masthead page.

(36) Dubois, D. L.; Mason, R.; Meek, D. W.; Scollary, G. R. *J. Organomet. Chem.* **1976**, *114*, C30.

(37) Jacobson, R. A.; Karcher, B. A.; Montag, R. A.; Socol, S. M.; Vande Griend, L. J.; Verkade, J. G. *Phosphorus Sulfur* **1981**, *11*, 27 and references cited therein.

Contribution from the Laboratoire d'Etude des Solutions Organiques et Colloidales, UA CNRS 406, Université de Nancy I, 54506 Vandoeuvre-les-Nancy Cedex, France

Carbon-13 and Proton Relaxation in Paramagnetic Complexes of Amino Acids. Structure and Dynamics of Copper(II)-L-Histidine (1:2) in Aqueous Solution

Bernard Henry, Jean-Claude Boubel, and Jean-Jacques Delpuech*

Received March 25, 1985

The ^{13}C relaxation times T_1 and T_2 and the isotropic shifts of 0.95 M aqueous solutions of L-histidine at pH 10.5 (or pD 10.9) containing ca. 10^{-3} M copper(II) perchlorate are measured at 62.86 MHz over a temperature range of 20-70 °C. T_1 is shown to be purely dipolar and controlled by the tumbling rate of the complex, while T_2 is purely scalar and controlled by both ligand exchange and electronic relaxation. This allows us to extract carbon-to-metal distances, using the known geometry of the imidazole ring and hyperfine coupling constants: A_C = 1.60, -1.65, 0.37, 0.92, and 2.05 MHz for C_1, C_2, C_3, C_4, and C_6, respectively. Dynamic parameters were preferably extracted from the ^1H NMR of proton H_6 at 250 MHz, yielding the tumbling correlation time $\tau_R(25\ °C) = 1.25 \times 10^{-10}$ s, the L-histidine exchange rate $k_M(25\ °C) = 7.46 \times 10^5\ s^{-1}$ (and the corresponding activation parameters, $\Delta H^* = 9.4$ kcal mol^{-1} and $\Delta S^* = 0.0$ eu), and the electronic relaxation time $T_{1e} = 0.92 \times 10^{-9}$ s. The structure of the complex in solution most likely involves two tridentate histidine molecules. The T_{1e} value is shown to be in reasonable agreement with the one computed from ESR data and the above τ_R value, showing the predominant contribution of spin-rotation interaction compared to the effect of **g** and **A** tensor anisotropy.

Introduction

Copper complexes play an essential role in biochemistry and pharmacology. Certain copper(II)-protein complexes serve as enzymes required by all cells in the human body for normal metabolic processes.[1] Transport of copper(II) in blood is vital to maintaining its concentration at a constant level. It has been shown that copper(II) was bound under physiological conditions

(1) Frieden, E. In "Metal Ions in Biological Systems"; Sigel, H., Ed.; Marcel Dekker: New York, 1981; Vol. 13, Chapter 1.

0020-1669/86/1325-0623$01.50/0

to either an amino acid, L-histidine,[2,3] or a macromolecule, serum albumin[4] (HSA) (where again the Cu(II) binding primarily involves a histidine residue[5]). Copper(II) may be released from the Cu(II)–L-His_2 complex to HSA by the formation of a ternary complex, Cu(II)–HSA–His,[6,7] and then from the HSA complex to the tissues. Copper(II) deficiency as well as the presence of excess ion results from genetically controlled diseases, known as the Wilson's[8] or Menke's diseases,[9] respectively. In the latter case, incorporation of copper(II) is performed by intravenous administration of the Cu(II)–L-His_2 complex.[2] All these facts account for the exceptional importance of knowing the exact mode of histidine chelation of copper(II) in Cu(II)–L-His_2 complexes and the kinetic behavior of the ligand exchange.

In spite of many efforts, the structures of copper(II)–L-histidine complexes are far from being elucidated. Potentiometric measurements show the presence of a variety of species in aqueous solution,[10] depending on the pH.[3,11-13] At neutral pH, only one species seems to exist in aqueous solution, namely the MA_2 complex, where A represents the completely deprotonated ligand and M the Cu^{2+} cation (in acidic medium, however, other species are simultaneously present, involving one or two monoprotonated molecules). This point seems to be confirmed by UV, CD,[14,15] and infrared[3] or Raman data.[16] In spite of this apparent simplicity at neutral pH, a great variety of structures have been proposed for the MA_2 complex according to the mode of histidine chelation of copper. Depending on the pH, histidine molecules may act as (a) bidentate ligands (LL) bound to copper(II) through amino N and carboxyl O atoms (glycine-like bonding), (b) bidentate ligands (LL′) bound to copper(II) through amino and imidazole N's (histamine-like bonding), or else (c) tridentate ligands with N's in the square plane and carboxyl O chelated axially (on steric grounds, the three donor atoms cannot all occupy a planar site simultaneously).

It is generally admitted that copper(II) ions prefer a square-planar or distorted octahedral geometry allowing a maximum of two amino acid ligands, eventually completed with one or two water molecules in an axial position.[16] The MA_2 complex may then be represented by formulas associating two of the three possible histidine chelates LL, LL′, or LLL. Six combinations are possible, all of which have been proposed successively in various publications (Figure 1). Unfortunately the X-ray diffraction solid-state structure is not presently available since all attempts to crystallize the Cu(II)–L-His_2 complex at neutral pH have been unsuccessful. Four related structures have however been reported, the crystal structures of (a) the complex Cu(II)–L-His_2 crystallized at pH 3.7, of the type $Cu^{II}(LL)_2(H_2O)_2$[18], (b) a complex consisting of Cu(II) bound to a tridentate L-histidine and a bidentate L-threonine[21] or L-asparagine[22] at physiological pH, suggesting that

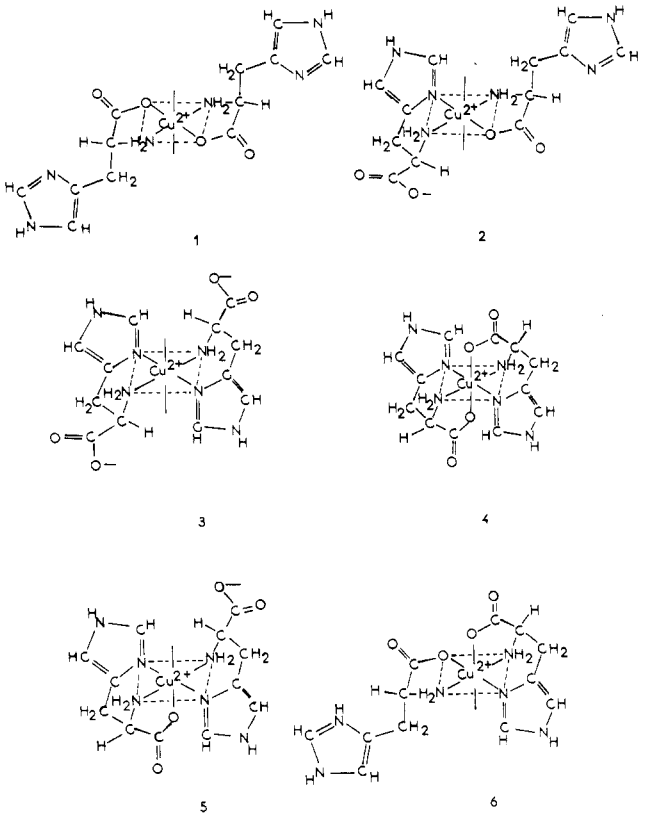

Figure 1. The six formulas for the Cu(II)–L-His_2 complex: (**1**) $Cu^{II}(LL)_2(H_2O)_2$;[16-18] (**2**) $Cu^{II}(LL)(LL')(H_2O)_2$;[19] (**3**) $Cu^{II}(LL')_2(H_2O)_2$;[20] (**4**) $Cu^{II}(LLL)_2$;[3,21,22] (**5**) $Cu^{II}(LLL)(LL')(H_2O)$;[3,15,21] (**6**) $Cu^{II}(LLL)(LL)(H_2O)$.[23]

the Cu(II)–L-His_2 complex itself is of the type $Cu^{II}(LLL)_2$ or $Cu^{II}(LL')(LLL)H_2O$, (c) the Cu(II)–L-His-D-His complex[20] of the type $Cu(LL')_2(H_2O)_2$.

A Raman scattering study[16] of the Cu(II)–L-His_2 complex confirms a chelated structure in which the two nitrogen atoms of the amino group and the two nitrogen atoms of the imidazole rings are bound to the Cu(II) ion in a square-planar trans position, as initially proposed by Kruck and Sarkar.[3] However the latter study also points to the presence of at least one carboxylato group bound in the axial position, this involves a structure of the type $Cu^{II}(LLL)(LL')H_2O$.

In this paper, we present additional information from ^{13}C and ^{1}H NMR measurements. Although paramagnetic probes are currently used in biology, NMR investigations of copper(II) complexes seem to be much less common than those involving, e.g., cobalt(II) or manganese(II) ions. Detailed carbon-13 relaxation data have been reported in the literature for a few systems only, such as the hexahydrate ion[24-29] or complexes with pyridines[30] or acetylacetonate.[31] As far as copper(II)–peptide systems are concerned, two studies only seem to have been reported to date, namely the Cu(II)–L-Pro_2[32] and the Cu(II)–Asp-Ala-His-NCH_3 complexes.[33] In the latter case, the presence of both dipolar and scalar contributions to ^{13}C relaxation rates precluded interpretation of distances on the basis of selective line-broadenings. In the first

(2) Sarkar, B. In "Metal Ions in Biological Systems"; Sigel, H., Ed.; Marcel Dekker: New York, 1981; Vol. 12, Chapter 6.
(3) Kruck, T. P. A.; Sarkar, B. *Can. J. Chem.* **1973**, *51*, 3549, 3563.
(4) Bearn, A. G.; Kunkel, H. G. *Proc. Soc. Exp. Biol. Med.* **1954**, *85*, 44.
(5) Appleton, D. W.; Sarkar, B. *J. Biol. Chem.* **1971**, *246*, 5040.
(6) Sarkar, B.; Wigfield, Y. *Can. J. Biochem.* **1968**, *46*, 601.
(7) Lau, S.; Sarkar, B. *J. Biol. Chem.* **1971**, *246*, 5938.
(8) Wilson, S. A. K. *Brain* **1912**, *34*, 295.
(9) Menke, J. H.; Alter, H.; Steigleder, G. K.; Weakley, D. R.; Sung, J. H. *Pediatrics* **1962**, *29*, 764.
(10) Sundberg, R. J.; Martin, R. B. *Chem. Rev.* **1974**, *74*, 471.
(11) Freeman, H. C.; Martin, R. P. *J. Biol. Chem.* **1969**, *244*, 4824.
(12) Morris, P. J.; Martin, R. B. *J. Inorg. Nucl. Chem.* **1970**, *32*, 2891.
(13) Childs, C. W.; Perrin, D. D. *J. Chem. Soc. A* **1969**, 1039.
(14) (a) Casella, L.; Gullotti, M. *J. Inorg. Biochem.* **1983**, *18*, 19. (b) Casella, L.; Gullotti, M. *Inorg. Chem.* **1983**, *22*, 242. (c) Casella, L.; Gullotti, M. *Inorg. Chem.* **1985**, *24*, 84.
(15) Wilson, E. W.; Kasperian, M. H.; Martin, R. B. *J. Am. Chem. Soc.* **1970**, *92*, 5365.
(16) Itabashi, M.; Itoh, K. *Bull. Chem. Soc. Jpn.* **1980**, *53*, 3131.
(17) Sarkar, B.; Wigfield, Y. *J. Biol. Chem.* **1967**, *242*, 5572.
(18) Evertsson, B. *Acta Crystallogr., Sect. B: Struct. Crystallogr. Cryst. Chem.* **1969**, *B25*, 30.
(19) Sigel, H.; McCormick, D. B. *J. Am. Chem. Soc.* **1971**, *93*, 2041.
(20) Camerman, N.; Fawcett, J. K.; Kruck, T. P. A.; Sarkar, B.; Camerman, A. *J. Am. Chem. Soc.* **1978**, *100*, 2690.
(21) Freeman, H. C.; Guss, J. M.; Healy, M. J.; Martin, R. P.; Nockolds, C. E.; Sarkar, B. *J. Chem. Soc. D* **1969**, 225.
(22) Ono, T.; Shimanouchi, H.; Sasada, Y.; Sakurai, T.; Yamauchi, O.; Nakahara, A. *Bull. Chem. Soc. Jpn.* **1979**, *52*, 2229.
(23) Wellman, K. M.; Wong, B. K. *Proc. Natl. Acad. Sci. U.S.A.* **1969**, *64*, 824.
(24) Swift, T. J.; Connick, R. E. *J. Chem. Phys.* **1962**, *37*, 307.
(25) McCain, D. C.; Myers, R. J. *Mol. Phys.* **1974**, *28*, 1109.
(26) Morgan, L. O.; Nolle, A. W. *J. Chem. Phys.* **1959**, *31*, 365.
(27) Luz, Z.; Shulman, R. G. *J. Chem. Phys.* **1965**, *43*, 3750.
(28) Lewis, W. B.; Alei, M., Jr.; Morgan, L. O. *J. Chem. Phys.* **1966**, *44*, 2409.
(29) Poupko, R.; Luz, Z. *J. Chem. Phys.* **1972**, *57*, 3311.
(30) Boyer, A.; Fazakerley, V. *J. Inorg. Nucl. Chem.* **1981**, *43*, 1955.
(31) McGarvey, B. R. *J. Phys. Chem.* **1956**, *60*, 71.
(32) Henry, B.; Boubel, J.-C.; Delpuech, J.-J. *Polyhedron* **1985**, *4*, 1069.
(33) Laussac, J. P.; Sarkar, B. *J. Biol. Chem.* **1980**, *255*, 7563.

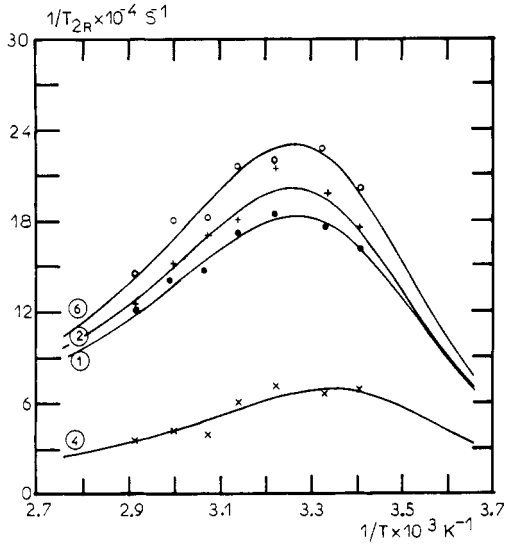

Figure 2. Temperature variations of the specific relaxation rate $1/T_{2r} = (1/T_2^{obsd} - 1/T_{2D})/p_M$ for the L-histidine carbons at 62.86 MHz, obtained from 0.95 M solutions of L-histidine in D_2O at pH 10.9 and with $[Cu^{2+}]$ = (0–3) *me 10^{-4} M: (●) C_1; (+) C_2; (×) C_4; (○) C_6. The curves were computed by using the parameters in Tables I, II, and IV, and correspond to the best fit.

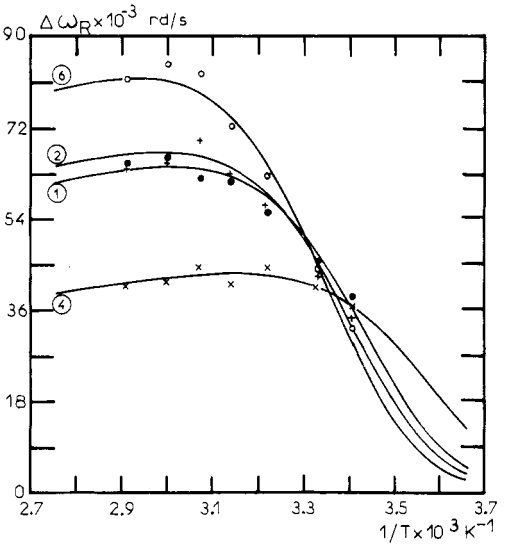

Figure 3. Temperature variations of the specific paramagnetic shift $\Delta\omega_r = (\omega_{obsd} - \omega_D)/p_M$ of the L-histidine carbons at 62.86 MHz, using the same conditions and notations as in Figure 2.

example,[32] we used a methodology worked out in this laboratory[34,35] to extract structural and kinetic parameters from ^{13}C and ^1H chemical shifts and relaxation times T_1 and T_2. We now extend this methodology to the case of the Cu(II)–L-His_2 complex.

Experimental Section

L-Histidine and hydrated copper(II) perchlorate $Cu(ClO_4)_2 \cdot 4H_2O$ were obtained from Bachem Feinchemikalien and Fluka, respectively, and were used without further purification. Concentrations C_M = 0, 3.0 × 10^{-5}, 5.0 × 10^{-5}, 10.0 × 10^{-5}, 20.0 × 10^{-5}, and 30.0 × 10^{-5} M (^{13}C NMR) and C_M = 0, 1.0 × 10^{-4}, 2.0 × 10^{-4}, 3.0 × 10^{-4}, 5.0 × 10^{-4}, 10.0 × 10^{-4} M (^1H NMR) of the Cu(II) cation and a fixed concentration C_A = 0.95 M of L-histidine were used in this study. Solutions were added with deuterated soda NaOD to obtain pD 10.9. Potentiometric measurements were carried out with a Methrom EA436 potentiometer and a combined glass–calomel Ingold microelectrode. All samples were prepared in a nitrogen atmosphere with water that has been purged with nitrogen and NMR tubes equipped with tight-fitting caps. The magnetic susceptibility of the complex, μ_M = 2.02 μ_B, in water solution was measured according to the method first described by Evans[36] and then by Crawford and Swanson.[37] Longitudinal relaxation times of ^{13}C nuclei are obtained from partially relaxed Fourier transform spectra by the use of CAMECA 250 spectrometer at 62.86 MHz or a Bruker WP-80 spectrometer at 20.1 MHz, with D_2O as an internal heteronuclear lock, a 180°–τ–90° pulse sequence, and the fast inversion–recovery variant.[38] Transverse relaxation times (^{13}C and ^1H) are obtained from line broadenings, $\Delta\nu$, measured at half-width on the spectra (62.86 and 250 MHz, respectively). Specific relaxation rates, $1/T_{ir} = (1/T_i - 1/T_{iD})/P_M$ (i = 1, 2), are obtained from the slope of the least-squares lines representing the relaxation rates $1/T_1$ and $1/T_2$ measured as a function of the fraction of the bound ligand, $p_M = 2C_M/C_A$ (T_{iD} represents the T_i value in the absence of the Cu(II) ion). T_1 and T_2 values of ^{13}C nuclei were determined at two (37 and 60 °C) and seven (20, 27, 37, 45, 52, 60, and 70 °C) temperatures, respectively. T_2 values of ^1H nuclei were measured at ten temperatures (5, 8, 9.5, 15, 20, 25, 35, 45, 55, and 71 °C). All calculations were performed on a Texas Instruments 980A minicomputer equipped with a Hewlett-Packard 7210A digital plotter.

Determination of Structural and Kinetic Parameters

Structural parameters were obtained from T_1 and T_2 relaxation times and paramagnetic shifts $\Delta\omega$ of C_1–C_6 of bound histidine molecules (for numbering, see Figure 5). Kinetic parameters were also obtained from the treatment of ^{13}C data, but a better accuracy was achieved from T_2 and $\Delta\omega$ measurements of proton H_6. Experiments were carried out in D_2O solutions at pD 10.9 for concentrations in the range $[Cu^{2+}]$ = 0–10^{-4} M (^{13}C) or 0–10^{-3}

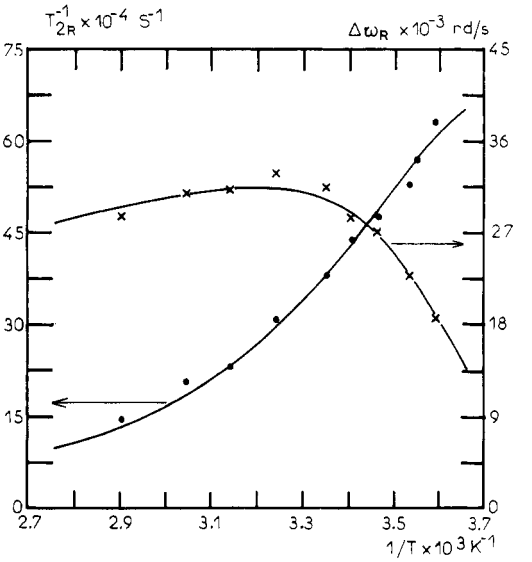

Figure 4. Same plots as in Figure 2 (●) and 3 (×) for proton H_6 of a 0.95 M L-histidine solution with $[Cu^{2+}]$ = 0–10^{-3} M.

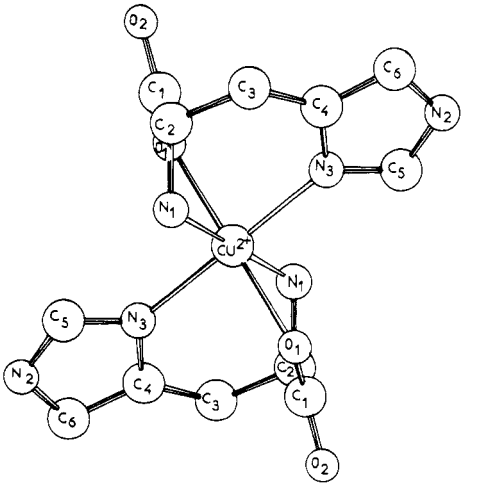

Figure 5. Structure of the copper(II)–L-histidine complex in D_2O solution at pD 10.9 and T = 37 °C.

(34) Henry, B.; Rappeneau, M.; Boubel, J.-C.; Delpuech, J.-J. *Adv. Mol. Relax. Interact. Processes* **1980**, *16*, 29.
(35) Henry, B.; Boubel, J.-C.; Delpuech, J.-J. *Polyhedron* **1982**, *1*, 113.
(36) Evans, D. F. *J. Chem. Soc.* **1959**, 2003.
(37) Crawford, T. H.; Swanson, J. *J. Chem. Educ.* **1971**, *48*, 382.
(38) Canet, D.; Levy, G. C.; Peat, I. R. *J. Magn. Reson.* **1975**, *18*, 199.

M (^{1}H) and [L-histidine] = 0.95 M. Under these conditions, there was a slow deuteration on C_5, precluding measurements in this position at higher temperatures. In this pH range, the Cu(II) cation is bound to the amino acid under the form of a single bis(L-histidine)copper(II) complex (see above). Carbon or hydrogen nuclei may therefore exist either in a diamagnetic or a paramagnetic site respectively (these two sites are denoted D and M in the following), assuming that both histidine ligands occupy equivalent positions in the Cu(II) complex. Ligand exchange is fast at high temperature (60 °C) and intermediate at lower temperature. The measured nuclear parameters T_1, T_2, and $\Delta\omega$ therefore depend on their values in the paramagnetic site (T_{1M}, T_{2M}, $\Delta\omega_M$) and in the diamagnetic site (T_{1D}, T_{2D}, $\Delta\omega_D$) and on the exchange rate $1/\tau_M$ of the bound histidine molecule. Extracting T_{1M}, T_{2M}, $\Delta\omega_M$ and $1/\tau_M$ from the experimentally observed quantities T_1, T_2, and $\Delta\omega$ is the first point of these investigations.

Theoretical expressions relating $\Delta\omega$, $1/T_1$, and $1/T_2$ to p_M and T are well-known at the present time.[39] The set of theoretical equations used in this paper (eq 1–9) starts from the Swift–Connick equations[24] for two exchanging sites:

$$1/T_{1r} = (1/T_1 - 1/T_{1D})/p_M = 1/(T_{1M} + \tau_M) \quad (1)$$

$$1/T_{2r} = (1/T_2 - 1/T_{2D})/p_M = \left(\frac{1}{\tau_M}\right)\frac{1/T_{2M}^2 + 1/T_{2M}\tau_M + \Delta\omega_M^2}{(1/T_{2M} + 1/\tau_M)^2 + \Delta\omega_M^2} \quad (2)$$

$$\Delta\omega_r = \Delta\omega/p_M = \frac{\Delta\omega_M}{(1 + \tau_M/T_{2M})^2 + \tau_M^2\Delta\omega_M^2} \quad (3)$$

These equations are just as valid for slow as for fast or intermediate exchange rates, provided that they apply to one predominant site (D), the observed line, exchanging with one (or several) sites (M) actually not detected in the spectrum. Specific relaxation rates and paramagnetic shifts, $1/T_{1r}$, $1/T_{2r}$, and $\Delta\omega_r$, are obtained from least-squares plots of $1/T_1$, $1/T_2$, or $\Delta\omega$ vs. p_M, respectively. Straight lines were effectively obtained in any case with correlation coefficients always larger than 0.995. Outer-sphere contributions were taken as negligible, as is always the case in such investigations, due to (i) the absence of contact interaction beyond the first solvation shell and (ii) the strong decrease of dipolar contributions as a consequence of the $1/r^6$ law (decreasing this contribution to 1.5% by approximately doubling the electron-to-nucleus distances in the outer sphere) and also of the presence of a majority of water molecules in the second coordination sphere.

In a second step, the intermediate parameters τ_M, T_{1M}, T_{2M}, and $\Delta\omega_M$ are expressed as a function of the temperature T and the resonant frequencies ω_C (or ω_H) of carbon (or hydrogen) nuclei and of the unpaired electron ω_e. τ_M is assumed to obey an Arrhenius law

$$\tau_M = \tau_M^\circ \exp(E_M/RT) \quad (4)$$

$\Delta\omega_M$ is related to the hyperfine coupling constant A through the equation

$$\Delta\omega_M/\omega = 2\pi A\mu_M(S(S+1))^{1/2}/3kT\gamma \quad (5)$$

Relaxation rates in the paramagnetic site are expressed by classical equations relating $1/T_{1M}$ and $1/T_{2M}$ to ω_e, ω_C (or ω_H), τ_R, and T_{1e}.[40]

These expressions are greatly simplified in the present case where τ_M ($\sim 10^{-6}$ s) >> T_{1e} ($\sim 10^{-8}$ s) >> τ_R ($\sim 10^{-10}$ s), and $\omega_e^2T_{1e}^2$ and $\omega_e^2\tau_R^2$ >> 1:

$$1/T_{1M} = \frac{2 \times 10^{-14}}{5}\left(\frac{\mu_M^2\gamma^2}{r^6}\right)\tau_R \quad (6)$$

$$1/T_{2M} = 7/6(1/T_{1M}) + 4\pi^2A^2S(S+1)T_{1e}/3 \quad (7)$$

(assuming that pseudocontact interaction makes a negligible contribution to the overall hyperfine coupling constant, see the discussion below). τ_R is again assumed to obey an Arrhenius law

$$\tau_R = \tau_R^\circ \exp(E_R/RT) \quad (8)$$

The electron relaxation rate may be shown to be inversely proportional to the reorientation correlation time

$$1/T_{1e} = K/\tau_R \quad (9)$$

where the constant K is independent of T and ω (see the discussion below).

Structural information then arises from eq 6 applied to carbon-13 nuclei. A first adjustment of the unknown parameters appearing in eq 1–9 has then been performed by using exclusively ^{13}C data. These parameters may be divided into two classes, those which refer to the whole complex (τ_M°, E_M°, τ_R°, E_R°, K) and those which are specific to each ^{13}C nucleus characterized by its own electron-to-nucleus distance r_{C_i} (i = 1–6) and hyperfine coupling constant A_{C_i}.

In a first cycle of computation, all the adjustable parameters are given an approximate value (denoted by superscript 1 in the following). Longitudinal relaxation rates $1/T_{1r}$ allow us to obtain approximate T_{1M} values if we neglect τ_M with respect to T_{1M} in eq 1 ($\tau_M << T_{1M}$). The knowledge of T_{1M} values for C_3–C_6 assumed to form a basis of known geometry (the imidazole ring including C_3 is planar as shown by X-ray diffraction studies[18,20–22,41]) allows us to position the Cu^{2+} ion with respect to the imidazole ring according to a procedure that has been fully explained in previous papers.[34,35] This procedure is based on the consideration of the three ratios

$$\lambda_{ij}^6 = (r_{C_j}/r_{C_i})^6 = \frac{T_{1M}^{(1)}(C_j)}{T_{1M}^{(1)}(C_i)}$$

with i = 3–6 and j = 3–6. The Cu^{2+} ion is therefore located on three spheres S_{ij} whose diameters M_iM_j are determined by the two points M_i and M_j, which share the internuclear vector C_iC_j in a known ratio λ_{ij}. The position of the copper(II) nucleus results from the intersection of three spheres, S_{12}, S_{23}, and S_{34}. Two positions are actually obtained in this way; they are however symmetrical with respect to the imidazole plane in the present case, thus leading to the same overall complex (in fact the Cu^{2+} ion is found quite close to the imidazole plane itself). This allows us in turn to compute the distances between Cu^{2+} and the remaining carbons C_1 and C_2 and thus to locate these carbons with respect to the imidazole ring. In fact, the localization of carbons C_1 and C_2 was instead achieved in the present studies by using the crystallographic data relative to the above mentioned complexes in which the Cu^{2+} ion was found to be positioned with respect to the imidazole plane almost exactly as in the Cu^{2+}–L-His_2 complex presently studied (see the discussion below). The knowledge of the copper(II) to carbon distances allows us in turn to compute an approximate value $\tau_R^{(1)}$ of the reorientational correlation time from eq 6. Similar computations are also performed at 60 °C (Table I), yielding a second value that combined with the previous one at 37 °C allows us to deduce the Arrhenius parameters $\tau_R^{\circ(1)}$ and $E_R^{(1)}$. Approximate values of the hyperfine coupling constants $A_{C_i}^{(1)}$, with i = 1–6, are obtained by taking $\Delta\omega_M = \Delta\omega_r$ as a limiting expression for eq 3 at temperatures higher than 50 °C. $\tau_M^{(1)}$ and $T_{2M}^{(1)}$ at any temperature are then deduced from eq 2 and 3, which are recast under the following forms:

$$1/T_{2M} = \frac{\Delta\omega_M(1/\tau_M - 1/T_{2r}) - \Delta\omega_r/\tau_M}{\Delta\omega_r} \quad (2a)$$

$$\Delta\omega_M = \frac{\Delta\omega_r}{(1 - \tau_M/T_{2r})^2 + \tau_M^2\Delta\omega_r^2} \quad (3a)$$

Four $\tau_M^{(1)}$ values can be computed in this way, and the value

(39) (a) For a review, see: Dwek, R. A. "NMR in Biochemistry: Application to Enzyme Systems"; Clarendon Press: Oxford, England, 1973. (b) Chachaty, C.; Rigny, P. *J. Chim. Phys.* **1982**, *79*, 203.

(40) Carrington, A.; McLachlan, A. D. "Introduction to Magnetic Resonance"; Harper and Row: New York, 1967.

(41) Madden, J. J.; McGandy, E. L.; Seeman, N. C. *Acta Crystallogr., Sect. B: Struct. Crystallogr. Cryst. Chem.* **1972**, *B28*, 2377.

Table I. Relaxation Rates T_{1M}^{-1} (s^{-1}) of ^{13}C Nuclei in Bound L-Histidine Molecules[a] and the Distances r (Å) between the Cu(II) Cation and the Atoms of L-Histidine in the Complex Cu(II)–L-His_2[b]

	37 °C		60 °C	
atom	T_{1M}^{-1}	r	T_{1M}^{-1}	r
C_1	1400 ± 50	2.89 ± 0.12	742 ± 30	2.83 ± 0.11
	(1332 ± 58)	(2.97 ± 0.12)	(782 ± 34)	(2.89 ± 0.10)
C_2	1380 ± 48	2.90 ± 0.09	758 ± 30	2.82 ± 0.10
	(1297 ± 50)	(2.98 ± 0.12)	(753 ± 30)	(2.91 ± 0.10)
C_3	417 ± 20	3.50 ± 0.11	243 ● 15	3.42 ± 0.12
	(414 ± 21)	(3.56 ± 0.13)	(269 ± 15)	(3.46 ± 0.14)
C_4	843 ± 38	3.25 ± 0.12	431 ± 24	3.20 ± 0.12
	(815 ± 38)	(3.16 ± 0.13)	(443 ± 24)	(3.18 ± 0.13)
C_5	877 ± 90	3.24 ± 0.26		
C_6	126 ± 15	4.18 ± 0.14	73 ± 8	4.25 ± 0.15
	(160 ± 16)	(4.23 ± 0.15)	(72 ± 8)	(4.31 ± 0.14)

[a] Values in parentheses are for 20.1-MHz data; all other values were obtained at 62.86 MHz. All data are for an aqueous solution of the complex. [b] See Figure 5.

finally adopted results from their arithmetic mean. From the knowledge of $(T_{2M}^{(1)})^{-1}$ the scalar contribution $(T_{2M}^{(1)})_{RS}^{-1}$ to the overall transverse relaxation time is obtained by subtracting the dipolar contribution estimated as $^7/_6(1/T_{1M}^{(1)})$ (see eq 7)

$$(T_{2M}^{(1)})_{RS}^{-1} = 4\pi^2 A_C^2 S(S+1)T_{1e}/3 \qquad (7a)$$

(in fact the dipolar contribution was always found to represent less than 1% of the overall relaxation rate). The electronic relaxation time $T_{1e}^{(1)}$ is then obtained from eq 7a and, in turn, the constant $K^{(1)}$ from eq 9.

A least-squares optimization procedure is then started so as to obtain the best fit between the experimental and theoretical values of $1/T_{2r}$ as a function of T (Figure 2). In a first set of iterations, the parameters $A_C^{(1)}$ and $r_C^{(1)}$ are kept constant, while parameters $\tau_M°$, E_M, K, $\tau_R°$, and E_R are adjusted in the course of successive iterations, taking as initial values the above approximate set of parameters $\tau_M°^{(1)}$, $E_M^{(1)}$, $K^{(1)}$, $\tau_R°^{(1)}$, and $E_R^{(1)}$. Let $\tau_M°^{(2)}$, $E_M^{(2)}$, $K^{(2)}$, $\tau_R°^{(2)}$, and $E_R^{(2)}$ be the set of adjusted parameters at the end of this computational step. The whole set of computations is then started again by using a slightly modified value of the hyperfine coupling constant A_C until a best value is found by trial and error for A_C (ensuring an absolute minimum of the squares of the residuals of $1/T_{2r}$ values). This approach can be made easier if one decides to perform an auxiliary fit of the function $\Delta\omega_r(T)$ (Figure 3) in which all the parameters except A_C are given constant values equal to the above set $\tau_M°^{(2)}$, $E_M°^{(2)}$, etc. Four sets of parameters are actually obtained in this way, since we may choose to optimize individual hyperfine coupling constants A_{C_1}, A_{C_2}, A_{C_4}, or A_{C_6}. The differences are reasonably small (Table II), and the final values of these parameters are taken as the arithmetic mean.

Parallel experiments were performed by ^1H NMR spectroscopy using the T_{2r} and $\Delta\omega_R$ values of proton H_6 at 10 temperatures (Figure 4). Computations were carried out along the same lines as with ^{13}C data. $\Delta\omega_M$ was identified with $\Delta\omega_r$ at higher temperatures, allowing us to compute an initial value $A_H^{(1)}$ of the hyperfine coupling constant, and, in turn, of $\Delta\omega_M$ at any temperature. $\tau_M^{(1)}$ and $1/T_{2M}^{(1)}$ could then be deduced from eq 2a and 3a. The dipolar contribution (6.8×10^2 s^{-1} from eq 6 and 7) to the overall transverse relaxation rate (8.7×10^4 s^{-1} at 5 °C) is negligible at any temperature. The value of $1/T_{2M}^{(1)}$ then yields $T_{1e}^{(1)}$ and $K^{(1)}$ from eq 7 and 9. The six parameters $1/\tau_M°$, E_M, $\tau_R°$, E_r, K, and A_H can then be adjusted from the best fit of $1/T_{2r}$ and $\Delta\omega_2$ as a function of the temperature (Figure 4).

Results and Discussion

Structure of the Complex. Values of the longitudinal relaxation times T_{1M} together with the Cu^{2+}–^{13}C distances are displayed in Table I. The imidazole atomic coordinates, which serve as a basis for the computation of these distances, are taken from X-ray data relative to pure histidine[41] or to various Cu^{2+}–L-Histidine complexes.[18,20-22] Longitudinal relaxation rates are determined with an error of ca. 5%. Ratios such as λ_{ij} are then obtained with an error $\Delta\lambda_{ij}/\lambda_{ij}$ of 1.5%. Values $\lambda_{ij} \pm \Delta\lambda_{ij}$ are then introduced into the computer program to estimate all the possible sets of distances r_{C_3}, r_{C_4}, r_{C_5}, and r_{C_6}. Each of these distances is given in Table I as the mean over the eight sets resulting from the combinations of the λ_{34}, λ_{45}, and λ_{56} ratios, and the corresponding errors are estimated as the difference between the maximum and the minimum values obtained for each parameter.

These data will help us to decide between structures **1–6** of Figure 1. From the crystallographic data relative to copper(II) complexes mentioned above,[18,20,22] we have computed the Cu^{2+}–C distances of histidine ligands coordinated in either of the three modes (LL), (LL'), or (LLL). Let us assume as a working hypothesis that these three structural units are kept unchanged in any Cu(II)–L-His_2 complex containing two of them. For a complex containing two identically chelated histidine molecules, the Cu^{2+}–C distances found above for each structural unit also

Table II. Fitted Values of the Parameters $1/\tau_M°$ (10^{13} s^{-1}), $\tau_R°$ (10^{-14} s), E_M (kcal mol^{-1}), E_R (kcal mol^{-1}), and K (10^{22}) from Carbons C_1, C_2, C_4, and C_6 (and the Corresponding Mean Values) and from Proton H_6[a]

	C_1	C_2	C_4	C_6	mean	H_6
$1/\tau_M°$	1.02 ± 0.40	0.91 ± 0.50	1.37 ± 0.35	1.67 ± 0.40	1.24 ± 0.41	1.60 ± 0.20
E_M	10.58 ± 0.20	10.72 ± 0.20	10.30 ± 0.10	10.19 ± 0.10	10.45 ± 0.15	10.00 ± 0.20
$\tau_R°$	4.28 ± 0.60	2.95 ± 0.60	3.50 ± 0.30	3.28 ± 0.28	3.50 ± 0.44	3.20 ± 0.15
E_R	4.60 ± 0.20	4.60 ± 0.20	4.65 ± 0.10	4.96 ± 0.12	4.70 ± 0.15	4.90 ± 0.10
K	1.53 ± 0.30	1.39 ± 0.30	1.28 ± 0.20	1.13 ± 0.20	1.33 ± 0.25	1.45 ± 0.12

[a] Too low accuracy was achieved with carbons C_3 (due to paramagnetic chemical shifts being very small) and C_5 (because of a slow H/D exchange), which were thus rejected in this comparison.

Table III. Distances (Å) between the Cu(II) Cation and the Atoms of L-Histidine in Complexes **1–6** (See Figures 1 and 5) Compared to the Corresponding Values Derived from Our NMR Data and from X-ray Crystallography of the Solid Ni(II)–L-His_2 Complex[42]

atom	1[a]	2	3[b]	4[c]	5	6	NMR[d] values	solid[e] Ni(II)–L-His_2
C_1	2.74	3.02	3.97	3.00	3.44	2.85	2.93 ± 0.12	2.83
C_2	2.82	2.95	3.14	2.84	2.96	2.83	2.94 ± 0.10	2.84
C_3	4.17	3.55	3.28	3.38	3.33	3.63	3.53 ± 0.12	3.49
C_4	4.96	3.33	2.99	2.99	2.99	3.33	3.20 ± 0.13	3.13
C_5	7.29	3.37	3.03	2.94	2.98	3.30	3.24 ± 0.26	3.06
C_6	5.65	4.52	4.13	4.13	4.13	4.53	4.20 ± 0.15	4.27
N_1	1.98		2.03	1.99				2.10
N_2	5.67		1.99	1.95				2.09
N_3	6.60		4.14	4.08				4.21
O_1	1.95		5.12	2.36				2.11
O_2	3.80		3.80	4.21				4.03

[a] Computed from ref 18. [b] Computed from ref 20. [c] Computed from ref 22. [d] Computed as the arithmetic mean of distances r at 37 °C in Table I (62.86 and 20.1 MHz). [e] Ref 42.

Table IV. Parameters Derived from ^{13}C and ^{1}H NMR Paramagnetic Chemical Shifts and Relaxation Times

Hyperfine Coupling Constants (MHz)

$A_{C_1} = +1.60 \pm 0.30$; $A_{C_2} = -1.65 \pm 0.27$; $|A_{C_3}|^a = 0.37 \pm 0.06$; $A_{C_4} = +0.92 \pm 0.12$; $A_{C_6} = +2.05 \pm 0.30$; $A_{H_6} = +0.68 \pm 0.02$

Reorientation Correlation Times

$\tau_R(25\ °C) = (1.03 \pm 0.37) \times 10^{-10}$ and $(1.25 \pm 0.25) \times 10^{-10}$ s
$\tau_R° = (3.50 \pm 0.44) \times 10^{-14}$ and $(3.20 \pm 0.25) \times 10^{-14}$ s
$E_R = 4.70 \pm 0.15$ and 4.90 ± 0.10 kcal mol^{-1}
(from ^{13}C and ^{1}H NMR data, respectively)

Electronic Relaxation Parameters

$T_{1e}(25\ °C) = (8.27 \pm 4.62) \times 10^{-9}$ and $(9.18 \pm 2.6) \times 10^{-9}$ s
$K = (1.33 \pm 0.25) \times 10^{22}$ and $(1.45 \pm 0.12) \times 10^{22}$
(from ^{13}C and ^{1}H NMR data, respectively)

Kinetic Parameters (from ^{1}H NMR)

$\tau_M(25\ °C) = 1.34 \times 10^{-6}$ s or $k_M = 7.46 \times 10^5$ s^{-1}
$1/\tau_M° = (1.60 \pm 0.20) \times 10^{13}$ s^{-1}
$E_M = 10.00 \pm 0.10$ kcal mol^{-1}
$\Delta H^{\ddagger} = 9.40 \pm 0.10$ kcal mol^{-1}
$\Delta S^{\ddagger} = 0.0 \pm 0.3$ eu

[a] Estimated value from experimental line width.

refer to structures **1**, **3**, or **4**, respectively. For a complex containing two nonequivalent histidine molecules, e.g. the complex $Cu^{II}(LL)(LL')(H_2O)_2$, each Cu^{2+}–C distance r_{C_i} is compute as an arithmetic mean, such as

$$1/r_{C_i}^6 = 0.5(1/r_{C_i(LL)}^6 + 1/r_{C_i(LL')}^6)$$

The full array of theoretical Cu^{2+}–C distances is displayed in Table III to be compared with the values deduced from our experiments. This comparison clearly shows that only structure **4** is compatible with all our data within the experimental uncertainties reported in Table I. The Cu^{2+}–C_1 distance is clearly compatible only with structures **2**, **4**, and **6**, among which only structure **4** can be retained after the following arguments. All the Cu^{2+}–C distances in structure **4** are not beyond the uncertainty range of NMR values by more than 0.08 Å, while the Cu^{2+}–C_6 distances in structures **2** and **6**, 4.52 and 4.53 Å, exceed the upper uncertainty boundary of the experimental NMR value (4.35 Å) by a significantly larger error of 0.17 Å. Moreover the Raman scattering study mentioned above, showing a planar arrangement of four nitrogen atoms points to the presence of structure **3**, **4**, or **5**, among which only *the bis tridentate complex, as proposed initially by Kruck and Sarkar,*[3] *is compatible with our NMR measurements.*

These distances are also in good agreement with those found from X-ray crystallography[42] in a closely related complex, Ni(II)-L-His_2, of the type $Ni^{II}(LLL)_2$. The distances of nitrogen and oxygen atoms to the metal ion are also given for convenience in Table III. The structure of the whole complex is represented in Figure 5 obtained from an ORTEP computer plot.[43]

Hyperfine Coupling Constants. An important point is to show that the dipolar contribution to the overall isotropic shift is negligible. Pseudocontact shifts δ_{pc} can be computed from the principal components $g_\parallel$ and $g_\perp$ of the **g** tensor after the formula[44]

$$\delta_{pc} = \frac{\bar{g}\beta^2 S(S+1)(g_\parallel - g_\perp)}{9kT}\left(\frac{3\cos^2\theta - 1}{r_C^3}\right) \qquad (10)$$

where $\bar{g} = (g_\parallel + 2g_\perp)/3$, β is the Bohr magneton, and θ is the angle between the tetragonal axis and the internuclear Cu^{2+}–C (or H) vector. Taking $r_c = 2.89$ Å for carbon 1 (Table I), $g_\parallel = 2.238$, and $g_\perp = 2.058$ from ESR data,[45] the pseudocontact shift at 25 °C amounts at most to ca. 5.5 ppm compared to an overall paramagnetic shift $\Delta\omega_M = 197$ ppm. Lower values are obtained for more remote carbons C_2–C_6 or for hydrogen H_6. This contribution can clearly be neglected, this validates the use of eq 5 to compute the A_C and A_H values reported in Table IV and eq 7 to compute the dynamic parameters of Tables II and IV.

Hyperfine coupling constants A_C thus represent the electron spin density ρ on the observed nucleus according to Fermi formula.[39b] In contrast with what is observed with the analogous Ni(II)-histidine complex,[46] the paramagnetic shift of the C_1 carbon atom assumes positive values at any temperature; this is consistent with the presence of one Cu(II)–L-histidine complex within the temperature and pH ranges explored. The values of ρ depend on spin delocalization and spin polarization through σ or π bonding. σ bonding may occur between the σ orbitals of the nitrogen atoms and the $d_{x^2-y^2}$ orbitals of the metal.[31,47] π bonding may be also envisaged with the presence of the imidazole plane and could account for the abnormally large A_C value for the most remote carbon C_6. However a similar observation has been made for the Cu(II)–L-proline complex,[32] in which the pyrrolidinic ring is substituted to the aromatic imidazole plane. Theoretical predictions seem therefore quite uncertain regarding the sign and magnitudes of hyperfine coupling constants. Negative A_C values for α-carbons C_2 have also been obtained for the Cu(II)–L-Pro_2[32] and Ni(II)–L-His_2[46] complexes, but not for the Mn(II) complexes with L-proline[35] and L-histidine.[48] Comparative data displayed in Table V also show that the larger hyperfine coupling constants seem to be associated with the copper(II) ion (as again compared to nickel(II) and manganese(II) ions).

Proton hyperfine coupling constants A_H are difficult to extract from ^{1}H NMR spectra due to line multiplicity and overlapping. This analysis was however possible for protons H_6 (Table IV) and H_5 in the histidine ring, where $A_H = 0.68$ and 0.57 MHz, respectively. The consideration of proton contact shifts is of importance to test the validity of the implicit assumption made throughout this work that unpaired electron spins are centered on the metal ion and can be regarded as point dipoles. Contributions from ligand-centered interactions to carbon-13 dipolar relaxation may however be important with respect to the above metal-centered interaction[61,62] especially for the histidine carbons, as pointed out by one reviewer. Theoretical treatments considering electron delocalization on ligand orbitals lead to the conclusion that carbon-13 relaxation rates should be proportional to the square of the hyperfine coupling constants A_H of attached protons in the case of predominant ligand-centered contribution. This is indeed not the case for the examined complex, since the ratio of relaxation rates $1/T_{1M}$ of C_5 and C_6 amounts to 6.96 (from data in Table I), while the corresponding A_H^2 ratio is only 0.70. This comparison strongly suggests the predominance of metal-centered interactions and validates the present treatments using the Solomon–Bloembergen equations.[40]

(42) Fraser, K. A.; Harding, M. M. *J. Chem. Soc. A* **1967**, 415.
(43) Johnson, C. K. "ORTEP", Report ORNL-3794; Oak Ridge National Laboratory: Oak Ridge, TN, 1965.
(44) Jesson, J. P. In "NMR of Paramagnetic Molecules"; La Mar, G. N., Horrocks, W. D., Holm, R. A., Eds; Academic Press: New York, 1973; Chapter 1.
(45) Cocetta, P.; Deiana, S.; Erre, L.; Micera, G.; Piu, P. *J. Coord. Chem.* **1983**, 12, 213.
(46) Led, J. J.; Grant, D. M. *J. Am. Chem. Soc.* **1977**, *99*, 5845.
(47) Kivelson, D.; Neiman, R. J. *J. Chem. Phys.* **1961**, *35*, 149.
(48) Led, J. J.; Grant, D. M. *J. Am. Chem. Soc.* **1975**, *97*, 6962.
(49) Swift, T. J.; Stephenson, T. A. *Inorg. Chem.* **1966**, *5*, 1100.
(50) Bernheim, A.; Brown, T. A.; Gutowsky, H. S.; Woessner, D. E. *J. Chem. Phys.* **1959**, *30*, 950.
(51) Boubel, J. C.; Delpuech, J.-J. *Mol. Phys.* **1974**, *27*, 113.
(52) Boubel, J.-C.; Brondeau, J.; Delpuech, J.-J. *Adv. Mol. Relax. Processes* **1977**, *11*, 323.
(53) Luz, Z.; Meiboom, S. *J. Chem. Phys.* **1964**, *40*, 2686.
(54) Breivogel, F. W., Jr. *J. Chem. Phys.* **1969**, *51*, 445.
(55) Lewis, W. B.; Morgan, L. O. In "Transition Metal Chemistry"; Carlin, R. L., Ed.; Marcel Dekker: New York, 1968; Vol. 4.
(56) Noack, M.; Kokoszka, G. F.; Gordon, G. *J. Chem. Phys.* **1971**, *54*, 1342.
(57) McConnell, H. M. *J. Chem. Phys.* **1956**, *25*, 709.
(58) (a) Kivelson, D. *J. Chem. Phys.* **1960**, *33*, 1094. (b) Wilson, R.; Kivelson, D. *J. Chem. Phys.* **1966**, *44*, 4440.
(59) Atkins, P. W.; Kivelson, D. *J. Chem. Phys.* **1966**, *44*, 169.
(60) McLachlan, A. D. *Proc. R. Soc London, Ser. A* **1964**, *A280*, 32.
(61) Doddrell, D. M.; Pegg, D. T.; Bendall, M. R.; Gottlieb, H. P. W.; Gregson, A. K.; Anker, M. *Chem. Phys. Lett.* **1976**, *39*, 65.
(62) Horrocks, W. D., Jr. In "NMR of Paramagnetic Molecules"; La Mar, G. N., Horrocks, W. D., Holm, R. A., Eds; Academic Press: New York, 1973; Chapter 4.

Table V. Hyperfine Coupling Constants (MHz) in Paramagnetic Complexes of L-Histidine and L-Proline

complex	carbon no. (or position) 1	2(α)	3(β)	4	5(δ)	6(γ)	ref
Mn(II)–L-Pro$_2$		1.6	0.8		2.2	2.5	35
Cu(II)–L-Pro$_2$		−1.95	0.42		1.7	1.9	32
Cu(II)–L-His$_2$	1.60	−1.65	0.37	0.92		2.05	this work
Mn(II)–L-His$_2$	0.43	0.2	0.12	0.60	1.07	0.41	48
Ni(II)–L-His$_2$	−0.15[a]	−0.36[a]	0.76[a]	1.25[a]	1.22[a]	0.54[a]	46
	0.43[b]	−1.39[b]	0.38[b]	0.65[b]	1.30[b]	1.51[b]	46

[a] Complex of the type $Ni^{II}(LLL)(LL')(H_2O)$. [b] Complex of the type $Ni^{II}(LLL)_2$; for nomenclature, see the text and Figure 1.

Table VI. Comparison of the Rate Constants and Activation Parameters for Ligand Exchange at 25 °C in Ni(II), Mn(II), and Cu(II) Complexes

	ligand/solvent H_2O/H_2O	Me_2SO/Me_2SO	MeOH/MeOH	L-Pro/H_2O	L-His/H_2O
		Ni^{2+}			
k, s^{-1}	6.33×10^4	1.14×10^4	1.0×10^3		7.14×10^3
$\Delta H^{\ddagger}$, kcal mol^{-1}	11.0	13.4	15.8		11.8
$\Delta S^{\ddagger}$, cal mol^{-1} K^{-1}	1.0	5.2	8.0		−1.4
ref	49	51	53		46
		Mn^{2+}			
k, s^{-1}	3.6×10^7	2.7×10^6	3.7×10^5	7.41×10^4	1.20×10^6
$\Delta H^{\ddagger}$, kcal mol^{-1}	7.8	8.9	6.2	15.6	13.2
$\Delta S^{\ddagger}$, cal mol^{-1} K^{-1}	2.9	0.7	−12	16.1	13.8
ref	50	52	54	35	48
		Cu^{2+}			
k, s^{-1}	5.6×10^9		1.0×10^8	4.00×10^5	7.16×10^5
$\Delta H^{\ddagger}$, kcal mol^{-1}	...		10.0	9.60	9.4
$\Delta S^{\ddagger}$, cal mol^{-1} K^{-1}	...		13	−0.7	0.0
ref	29		54	32	this work

Effective Electron Magnetic Moment. The value $\mu_M = 2.02 \pm 0.10\ \mu_B$ is in not too bad agreement with the value of 1.835 μ_B computed for an electron spin number $S = {}^1/_2$ and the above $g_\parallel$ and $g_\perp$ values mentioned above according to the formula

$$\mu_M^2 = (g_\parallel^2 + 2g_\perp^2)\beta^2 S(S+1)/3 \qquad (11)$$

As for the analogous copper(II)–L-proline complex,[32] the NMR value is somewhat larger than the one deduced from ESR measurements through eq 11, this may be due to $g_\parallel$ and $g_\perp$ values slightly modified by going from the solid state to aqueous solutions of the complex, and also to a second-order Zeeman (SOZ) contribution to the electronic magnetic moment, which is not given by the ESR experiments,[62] as pointed out by one reviewer.

Using effective electron magnetic moments to compute relaxation times T_{1M} (eq 6) implicity assumes an isotropic **g** tensor with an average value $g^2 = (g_\parallel^2 + 2g_\perp^2)/3$. As pointed out by one reviewer, due to **g** anisotropy the above value should be replaced, according to Sternlicht,[63] by

$$g'^2 = {}^1/_2[(g_\parallel^2 + 2g_\perp^2)/3 + g_\parallel^2 \cos^2\theta + g_\perp^2 \sin^2\theta]$$

in the case of an axially symmetric **g** tensor. This value may vary from one carbon nucleus to the next one, possibly vitiating all the distance ratios λ_{ij} mentioned above. In fact $g_\parallel \simeq g_\perp = g_e$, and the above two formulas converge to a common value $g = g' = g_e$. This can be checked in a second approximation using the atomic coordinates found previously. The ratio of relaxation times $T_{1M}(C_i)/T_{1M}(C_j)$ was found to be altered by 1.5% at most. This corresponds to alterations in the corresponding r_{C_j}/r_{C_i} ratio of at most 0.25%, which were then neglected in all discussions. Other recent theoretical treatments[64,65] considering the case of slowly rotating systems also lead to the conclusion of negligible contributions at the high frequencies used in this work.

Dynamic Information. Dynamic parameters result from four sets of adjusted parameters τ_M^0, E_M, τ_R^0, E_R, and K computed for each carbon atom C_1, C_2, C_4, and C_6. Final values of these parameters are given in Tables II and IV as arithmetic means over the four sets of data. They are compared with the ones obtained from ^1H NMR spectroscopy, which are thought to be more accurate, due to higher S/N ratios and larger paramagnetic shifts.

Tumbling correlation times were obtained in a first approach from longitudinal relaxation rates of carbon nuclei at two frequencies (Table I). These experiments show that extreme narrowing conditions ($\omega_C^2\tau_R^2 << 1$) are effectively fulfilled in the frequency range used in thus work. In a second run, adjusted parameters were obtained from transverse relaxation rates of ^{13}C nuclei at 62.86 MHz and proton H_6 at 250 MHz. Two values were thus obtained (Table IV), in good agreement with each other, τ_R (25 °C) = 1.03×10^{-10} and 1.25×10^{-10} s, respectively. They are closely similar to the ones previously found for Cu(II)–L-proline[32] and Mn(II)–L-proline[35] complexes (1.13×10^{-10} and 1.28×10^{-10} s). They are however somewhat smaller than the values obtained for the M(II)–L-histidine[48] and Ni(II)–L-histidine[46] complexes (5.64×10^{-10} and 4.80×10^{-10} s).

Kinetic parameters are best deduced from transverse relaxation rate measurements of proton H_6 (Table IV). For the sake of comparison, these values are reported in Table VI together with those relative to (i) the same ligand associated with metal ions commonly used as paramagnetic probes, Ni(II) and Mn(II), on the one hand, and (ii) systems involving either another amino acid, L-proline, or some solvents commonly used in biochemistry (H_2O, Me_2SO, MeOH), on the other hand. Rate constants k_M for ligand exchange in amino acid complexes seen to follow the same trend as for solvent exchange in the corresponding solvation complexes, namely

$$Ni^{2+} << Mn^{2+} \sim Cu^{2+}$$

In fact, chemical exchange on homogeneous hexacoordinated copper(II) complexes, such as $Cu(H_2O)_6^{2+}$, are known to be subject to Jahn–Teller effects, involving two different exchange rates for the axial and equatorial ligand molecules.[24,55] Difficulties of the same type could arise with copper(II) amino acid complexes, although Jahn–Teller effects are likely to be larger in the case

(63) Sternlicht, H. *J. Chem. Phys.* **1965**, *42*, 2250.
(64) Gottlieb, P. W.; Barfield, M.; Doddrell, D. M. *J. Chem. Phys.* **1977**, *67*, 3785.
(65) Banci, L.; Bertini, I.; Luchinat, C. *Chem. Phys. Lett.* **1985**, *118*, 345.

of the above homogeneous hexacoordinated complexes.[56] We may only say that one exchange rate only was necessary to obtain good theoretical fits throughout these experiments.

One may also notice that ligand exchange in L-proline complexes of Mn(II) and Cu(II) seems to follow the same sequence, $k_M(Mn^{2+}) < k_M(Cu^{2+})$, as the solvent exchange, even if the gap between the two sets of rate constants is much reduced in this case, while this sequence is in the reverse order for L-histidine complexes. For both L-histidine and L-proline complexes, a dramatic drop of activation parameters can be observed by going from Mn(II) to Cu(II) complexes. These results cannot be rationalized in the present state of these investigations.

One may wonder how the exchange time of a terdentate ligand may be as short as 10^{-6} s. It should however be emphasized that the NMR observation actually refers to the overall site exchange

$$Cu(LLL)_2 + LLL^* \overset{K}{\rightleftharpoons} Cu(LLL)(LLL)^* + LLL$$

with an equilibrium constant K equal to unity under any circumstance, and not to the formation/dissociation process[66] of the complex

$$Cu_{aq}^{2+} + LLL \overset{K_1}{\rightleftharpoons} Cu(LLL)_{aq}^{+}$$

$$Cu(LLL)_{aq}^{+} + LLL \overset{K_2}{\rightleftharpoons} Cu(LLL)_2$$

with $K_1 \simeq 10^{10}$ M^{-1} and $K_2 \simeq 10^8$ M^{-1}.

In fact, multidentate ligands can substitute to each other without the copper(II) ion being fully dissociated at any time. Ligand exchange then involves as a first step the fast reversible release of one end of the chelate as suggested by Lanier and Pearson[67] for solvent-assisted symmetrical exchange of glycine molecules on cations of transition metals. The evidence for such a fast preequilibrium was established on a firm basis by DNMR measurements of intramolecular optical inversion between the Λ and Δ enantiomers of D_3 tris complexes of diphosphorylated symmetrical bidentate ligands.[68] We showed in this case that the internal detachment–reattachement process was interrupted about one time out of one thousand by external ligand exchange.[69] Such mechanisms are probably still valid for terdentate ligands. They would involve the fast reversible release of one (or two) end(s) of a histidine molecule LLL in the complex, followed from time to time by the attachment of a third monodentate (or bidentate) histidine molecule LLL* from the bulk solution. Compared to the internal reattachment of LLL, the fixation of LLL* could take place one time out of one thousand, as mentioned above. This would explain that intermediate tridentate–bidentate–monodentate complexes such as

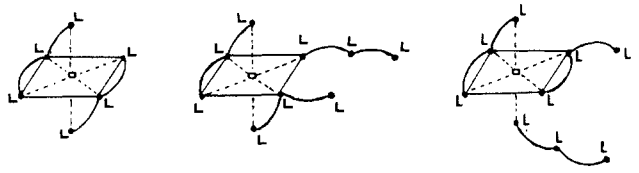

do not exist in a molar ratio larger than ca. $^1/_{1000}$ and thus do not contribute significantly to the overall paramagnetic relaxation. This step would be rate-determining for the whole ligand exchange with a time constant of ca. 10^{-5}–10^{-6} s, since the subsequent interchange between LLL and LLL* molecules around the Cu^{2+} ion may then proceed internally very fast.

Electronic Relaxation Times. Electronic relaxation is the fastest process determining the correlation time for scalar transverse relaxation rates of ^{13}C and ^1H nuclei in copper(II)–L-histidine complexes (Table IV). It is then of interest to compare the relaxation time T_{1e} derived from NMR measurements with the value that may be predicted from ESR data, as already shown in a previous publication.[32] Let us recall that for paramagnetic ions with $S = {}^1/_2$, ESR relaxation times depend on anisotropic hyperfine constants and the **g** tensor[57,58] and on spin–rotational effects.[59] These two contributions, $(1/T_{1e})_{g,A}$ and $(1/T_{1e})_{SR}$, respectively, can be expressed according to the approximate equations[57,59]

$$(1/T_{1e})_{g,A} = \frac{8\pi^2}{15}\left(\frac{(\Delta g)\beta B_0 + bI_z}{h}\right)^2\left(\frac{\tau_c}{1+\omega_e^2\tau_c^2}\right) \quad (12)$$

$$(1/T_{1e})_{SR} = \delta g^2/9\tau_R \quad (13)$$

where $\Delta g = g_\parallel - g_\perp = 0.180$, $B_0 = 5.87$ T, $b = A_\parallel - A_\perp$, with $A_\parallel$ and $A_\perp = 5.49 \times 10^8$ and 0.36×10^8 s^{-1}, respectively,[45] and $\delta g^2 = (g_\parallel - g_e)^2 + 2(g_\perp - g_e)^2$, with $g_e = 2.00233$. τ_c is the correlation time for the reorientation of the tetragonal axis bearing $g_\parallel$. This reorientation may be due either to molecular tumbling (in which case $\tau_c = \tau_R$) or to dynamical Jahn–Teller effects as discussed by Lewis and Morgan.[55] However, as mentioned above, Jahn–Teller effects are likely to occur only in the case of homogeneous hexacoordinated complexes,[56] such as the aquo complex.[28,29] We are then left with the first possibility and $\tau_c = \tau_R$. Observing that $\omega_e^2\tau_R^2 >> 1$, eq 12 can be reduced to

$$(1/T_{1e})_{g,A} = \frac{8\pi^2}{15}\left(\frac{1}{\omega_e^2\tau_R}\right)\left(\frac{(\Delta g)\beta B_0 + bI_z}{h}\right)^2 \quad (14)$$

I_z is the magnetic number of the copper nuclei, $I_z = \pm{}^3/_2, \pm{}^1/_2$, so that an average longitudinal relaxation rate $(1/T_{1e})_{g,A}$ has to be computed as the arithmetic mean over the four $(1/T_{1e})_{g,A}$ values obtained from eq 14, for each of the four I_z values.[29,60] Adding eq 14 and 15 together results in the expression of the overall electronic relaxation time

$$(1/T_{1e}) = (1/T_{1e})_{g,A} + (1/T_{1e})_{SR} = K/\tau_R \quad (15)$$

$$K = \delta g^2/9 + (8\pi^2/15h^2\omega_e^2)((\Delta g)^2\beta^2B_0^2 + b^2I(I+1)/3) \quad (16)$$

This explains the origin of eq 9 used to represent the electronic relaxation rate. With the values of $g_\parallel$ and $g_\perp$ quoted above,[45] the spin–rotational contribution is in fact predominant, $(1/T_{1e})_{SR} = 5.35 \times 10^7$ s^{-1} against $(1/T_{1e})_{g,A} = 8.60 \times 10^6$ s^{-1}, and $1/T_{1e} = 6.21 \times 10^7$ s^{-1} at 25 °C. The electronic relaxation time $T_{1e} = 1.60 \times 10^{-8}$ s thus computed from ESR data is relatively close to the one obtained from our NMR data, $T_{1e} = 0.92 \times 10^{-8}$ s. These values are also very close to the ones found for the analogous copper(II)–L-proline complex[32] ($T_{1e} = 1.18 \times 10^{-8}$ and 2.22×10^{-8} s from NMR and ESR data) and for the copper(II)-acetylacetonate complex[70] ($T_{1e} = 2.5 \times 10^{-8}$ s). They are larger by about 1 order of magnitude than the one measured for the aquo complex $Cu(H_2O)_6^{2+}$ from dynamic nuclear polarization experiments, $T_{1e} = 1.67 \times 10^{-9}$ s at 30 °C. This difference is probably due to smaller correlation times τ_R and larger Δg^2 and δg^2 values in eq 15 and 16.

Conclusion

The purely dipolar longitudinal relaxation contrasting with purely scalar transverse relaxation makes copper(II) a suitable paramagnetic probe to extract carbon-to-metal distances (through T_1 measurements of ^{13}C nuclei) and hyperfine coupling constants (from T_2 and shift measurements of ^{13}C and ^1H nuclei). The set of carbon-to-metal distances strongly favors the existence of a bis tridentate Cu(II)–L-His_2 complex in basic solutions. Dynamic parameters show a moderately fast ligand exchange. The rotational reorientation of the complex in turn controls the electronic relaxation rate. Using the components of the **g** and **A** tensors from

(66) Beattie, J. K.; Fensom, D. J.; Freeman, H. C. *J. Am. Chem. Soc.* **1976**, *98*, 500.
(67) Pearson, R. G.; Lanier, R. D. *J. Am. Chem. Soc.* **1964**, *86*, 765.
(68) Rubini, P. R.; Rodehüser, L.; Delpuech, J.-J. *Inorg. Chem.* **1979**, *18*, 2962.
(69) Doucet Ladevèze, G.; Rodenhüser, L.; Rubini, P. R.; Delpuech, J.-J. *Nouv. J. Chim.* **1984**, *8*, 93.
(70) Doddrell, D. M.; Pegg, D. T.; Bendall, M. R.; Gregson, A. K. *Chem. Phys. Lett.* **1976**, *40*, 142.

ESR data allows us to show that the electronic relaxation rate is dominated by spin–rotational interaction, thus making the electronic relaxation time directly proportional to the tumbling correlation time and almost independent of the magnetic field. This shows that higher magnetic field strengths can be used to advantage in the investigation of copper(II) complexes, since the improved chemical shift resolution thus obtained should not be canceled by significant extra line broadenings, an important point in the study of copper(II)–protein complexes.

Acknowledgment. Financial support from the Centre National de la Recherche Scientifique is gratefully acknowledged. All NMR spectra were recorded on spectrometers of the University of Nancy I.

Contribution No. 7199 from the Arthur Amos Noyes Laboratory of Chemical Physics, California Institute of Technology, Pasadena, California 91125

Preparation and Characterization of Pentanuclear Molybdenum Halide Clusters

Thomas C. Zietlow and Harry B. Gray*

Received May 30, 1985

The cyclic voltammogram of $[(n\text{-}C_4H_9)_4N]_2Mo_5Cl_{13}$ shows two quasi-Nernstian redox couples: $E_{1/2}(ox) = 0.49$ V and $E_{1/2}(red) = -0.36$ V vs. Ag/AgCl in methylene chloride solution. Both the electrochemically stable $Mo_5Cl_{13}^-$ and $Mo_5Cl_{13}^{3-}$ clusters have been isolated as their tetrabutylammonium salts. The synthesis of $[(n\text{-}C_4H_9)_4N]_2Mo_5Br_{13}$ is described along with its cyclic voltammogram, which also shows two quasi-Nernstian waves at $E_{1/2}(ox) = 0.41$ V and $E_{1/2}(red) = -0.33$ V [$(n\text{-}C_4H_9)_4NMo_5Br_{13}$ and $[(n\text{-}C_4H_9)_4N]_3Mo_5Br_{13}$ have been isolated]. The $[(n\text{-}C_4H_9)_4N]_3Mo_5X_{13}$ complexes are paramagnetic, and their temperature-dependent magnetic behavior is interpreted in terms of two thermally populated sublevels of a $^3A_2(e^2)$ ground state. Sublevel splittings of <4 cm^{-1} in $Mo_5Cl_{13}^{3-}$ and 15 (5) cm^{-1} in $Mo_5Br_{13}^{3-}$ are estimated from EPR data.

Our interest in the electronic structures of molybdenum(II) and tungsten(II) halide clusters began with the discovery of intense luminescence from $Mo_6Cl_{14}^{2-}$. The extremely long luminescent lifetime (180 μs in acetonitrile solution at room temperature)[1] and rich excited-state electron-transfer chemistry of this and analogous $Mo_6Br_{14}^{2-}$ and $W_6Cl_{14}^{2-}$ clusters[2] have led us to investigate the chemical and photochemical properties of the pentanuclear clusters of the $Mo_5Cl_{13}^{2-}$ type. Structurally, $Mo_5Cl_{13}^{2-}$ is a square pyramid of molybdenum atoms with four triply bridging chlorides on the faces of the pyramid, four chlorides bridging the basal molybdenum atoms, and five axial chlorides[3] (essentially the $Mo_6Cl_{14}^{2-}$ structure with one metal atom and its axial chloride removed). The open coordination site in these pentanuclear clusters could potentially facilitate ground- and excited-state multielectron-transfer reactions.

Here we report the preparation and the electronic spectroscopic, electrochemical, and magnetic properties of $(n\text{-}Bu_4N)Mo_5X_{13}$, $(n\text{-}Bu_4N)_2Mo_5X_{13}$, and $(n\text{-}Bu_4N)_3Mo_5X_{13}$ (X = Cl, Br) complexes. These experiments have allowed us to evaluate several key features of the Meissner–Korol'kov[4] electronic structural model for these clusters.

Experimental Section

Materials. The methylene chloride (Burdick and Jackson reagent grade) used in reactions and physical characterizations was dried over CaH_2, and vacuum-distilled onto 3-Å molecular sieves. All other materials were of reagent grade and used without further purification.

Cluster Compounds: $(n\text{-}Bu_4N)_2Mo_5Cl_{13}$ was prepared by the literature method[3] and recrystallized from methylene chloride/petroleum ether.

$(n\text{-}Bu_4N)_3Mo_5Cl_{13}$ was prepared by chemical reduction of $(n\text{-}Bu_4N)_2Mo_5Cl_{13}$ by stirring it over zinc metal in dry, deoxygenated methylene chloride solution. In a sample reaction $(n\text{-}Bu_4N)_2Mo_5Cl_{13}$ (100 mg) was dissolved in 30 mL of deoxygenated methylene chloride and stirred with a slight excess of n-Bu_4NCl and zinc for 24 h. The solution was filtered and petroleum ether distilled on top of the methylene chloride to crystallize the product. Recovery of the red crystals is about 80%. The solution is air-sensitive, but the crystals only slowly (days) decompose in air. Anal. Calcd for $C_{48}H_{108}N_3Mo_5Cl_{13}$: C, 34.56; H, 6.53; N, 2.52. Found: C, 34.57; H, 6.63; N, 2.53.

$(n\text{-}Bu_4N)Mo_5Cl_{13}$ was synthesized by chemical oxidation of $(n\text{-}Bu_4N)_2Mo_5Cl_{13}$ (100 mg) with chlorine in methylene chloride solution. The chlorine was removed from the reaction mixture by purging with argon and the blue solution was layered with petroleum ether to crystallize the product. Recovery of purple-blue crystals was 95%. Anal. Calcd for $C_{16}H_{36}NMo_5Cl_{13}$: C, 16.24; H, 3.07; N, 1.18. Found: C, 17.49; H, 3.43; N, 1.23.

$(n\text{-}Bu_4N)_2Mo_5Br_{13}$ was synthesized in a manner analogous to the chloride preparation. Aluminum bromide (6.2 g), potassium bromide (1.6 g), bismuth trichloride (1.1 g), bismuth (0.5 g), and potassium hexachloromolybdate(III) (0.5 g) were placed in a quartz tube that was evacuated and sealed off under vacuum. After 3 h of slow heating to 300 °C (*Caution! Explosion danger!*) and 1 h at 300 °C, the tube was allowed to cool to room temperature and broken, and the contents were extracted with 6 N HBr and filtered. The filtrate was treated with n-Bu_4NBr, causing a dull green precipitate to form. This was collected by vacuum filtration and dissolved in methylene chloride; this solution was dried over anhydrous $MgSO_4$ and crystallized with petroleum ether. The yield of crystalline material was 120 mg. Anal. Calcd for $C_{32}H_{72}N_2Mo_5Br_{13}$: C, 19.16; H, 3.59; N, 1.40; Mo, 23.95; Br, 51.90. Found: C, 19.39; H, 3.67; N, 1.49; Mo, 23.75; Br, 51.99.

$(n\text{-}Bu_4N)_3Mo_5Br_{13}$ was synthesized by reduction of $(n\text{-}Bu_4N)_2Mo_5Br_{13}$ in a manner completely analogous to that of the chloride. Both the light green solution and the crystals are air-sensitive. Anal. Calcd for $C_{48}H_{108}N_3Mo_5Br_{13}$: C, 25.67; H, 4.66; N, 1.87. Found: C, 25.19; H, 4.66; N, 1.90.

$(n\text{-}Bu_4N)Mo_5Br_{13}$ was also made in the same manner as the chloride, using bromine as the oxidant of the $(n\text{-}Bu_4N)_2Mo_5Br_{13}$. Crystallization of the methylene chloride solution with petroleum ether resulted in emerald green crystals.

Analytical Procedures. Carbon, hydrogen, nitrogen, molybdenum, and bromide were determined by Galbraith Microanalytical Labs, Inc.

Physical Measurements. Room-temperature magnetic susceptibility measurements were made on a Faraday balance with $HgCo(SCN)_4$ as calibrant. Variable-temperature susceptibility measurements were made at the University of Southern California on a SQUID-based (S.H.E. Corp.) Model 805 variable-temperature susceptometer with a 2 K option. Electronic spectra were recorded on a Cary 17 spectrometer. EPR spectra were measured on a Varian E-Line Century Series spectrometer equipped with an Air-Products Heli-Tran cooling system. Cyclic voltammetry was performed on a PAR model 174A polarographic analyzer with a Houston Instruments 2000 X-Y recorder. Controlled-potential electrolyses were performed with a Model 179 PAR potentiostat.

(1) Maverick, A. W.; Gray, H. B. *J. Am. Chem. Soc.* **1981**, *103*, 1298.
(2) Maverick, A. W.; Najdzionek J. S.; MacKenzie, D.; Nocera, D. G.; Gray, H. B. *J. Am. Chem. Soc.* **1983**, *105*, 1878.
(3) Jödden, K.; Schnering, H. G. v.; Schäfer, H. *Angew. Chem., Int. Ed. Engl.* **1975**, *14*, 570. Jödden, K.; Schäfer, H. *Z. Anorg. Allg. Chem.* **1977**, *430*, 5.
(4) Meissner, H.; Korol'kov, D. V. *Z. Anorg. Allg. Chem.* **1983**, *496*, 175.

0020-1669/86/1325-0631$01.50/0